Journal of Integrative Neuroscience

J. Integr. Neurosci. **2024**; 23(1): 14
https://doi.org/10.31083/j.jin2301014

Original Research

Heliox Protects SH-SY5Y Cells from Oxygen-Glucose Deprivation/Reperfusion-Induced Ferroptosis

Shuai Yu[1], Wei Xiong[1,*], Wanjing Xu[1], Yafen Chen[1]

[1]Department of Anesthesiology, Zhongshan Hospital, Xiamen University, 361004 Xiamen, China
*Correspondence: xiongwei200904@163.com (Wei Xiong)

Academic Editor: Hahn Young Kim
Submitted: 10 April 2023 Revised: 1 June 2023 Accepted: 13 June 2023 Published: 16 January 2024

Abstract

Background: Heliox shows protective effects against acute focal ischemia-reperfusion injury in the brain. However, further research is needed to unveil the intricate molecular mechanisms involved. Determining how heliox affects ferroptosis caused by oxygen-glucose deprivation/reoxygenation (OGD/R) in SH-SY5Y cells as well as the underlying mechanism was the goal of the current work. **Methods**: With the use of 2′,7′-Dichlorodihydrofluorescein diacetate (DCFH-DA), JC-1, and methyl thiazolyl tetrazolium, we assessed the survival, reactive oxygen species (ROS), and mitochondrial membrane potential in SH-SY5Y cells after they had been exposed to OGD/R and heliox. The expression of molecules associated with ferroptosis and the phosphatidylinositol 3-kinase/protein kinase B (PI3K/AKT) pathway was analyzed using quantitative polymerase chain reaction (PCR) and immunoblotting, while malondialdehyde (MDA), oxidized glutathione disulfide (GSSG), ferrous ion (Fe^{2+}), and reduced glutathione (GSH) levels were evaluated using biochemical kits. **Results**: OGD/R treatment reduced the GSH to GSSG ratio; the potential of the mitochondrial membrane; the expression of the proteins GSH, SLC7A11, and glutathione peroxidase 4 (GPX4); and the ability of SH-SY5Y cells to survive. In contrast, OGD/R treatment increased the expression of cyclooxygenase-2 (COX2), ACSL4, and ferritin heavy chain 1 (FTH1) proteins, the production of MDA and GSSG, and the levels of ROS and Fe^{2+}. However, heliox effectively mitigated all these OGD/R-induced effects. Furthermore, in OGD/R-treated SH-SY5Y cells, heliox administration stimulated the PI3K/AKT pathway while suppressing the nuclear factor-κB (NF-κB) pathway. When MK-2206, an AKT inhibitor, was applied concurrently to the cells, these outcomes were reversed. **Conclusions**: Heliox prevents OGD/R from causing ferroptosis in SH-SY5Y cells by activating the PI3K/AKT pathway. This suggests a promising therapeutic potential for heliox use in the management of ischemia/reperfusion injury.

Keywords: heliox; oxygen-glucose deprivation/reoxygenation; ferroptosis; PI3K/AKT pathway

1. Introduction

Ischemia/reperfusion (IR) occurs in several diseases and involves the two processes of ischemia and reperfusion [1]. Ischemia is linked to metabolic imbalance and cell hypoxia, while reperfusion, or reoxygenation of the ischemic area, induces an inflammatory response leading to tissue deterioration [2]. IR injury often occurs during this period and hinders patient recovery, although the mechanism of injury remains unclear. To manage IR injury, however, suppression of cell death has the potential to be a successful therapeutic approach.

Cell death encompasses necrosis, apoptosis, autophagy, and ferroptosis, and is essential to the pathogenesis of IR [3–5]. The two main types of cell death in IR injury are caspase-dependent apoptosis and necroptosis that is dependent on the activation of serine/threonine kinase-3 [6]. Although autophagy can maintain cell health, excessive autophagic activity during IR injury can induce neuronal death [6,7]. Ferroptosis characterized by severe lipid peroxidation and plasma membrane rupture, is another type of programmed cell death [8]. Ferroptosis-associated cellular events, including increased iron levels and lipid peroxidation, have been observed during IR injury [9–11]. Hence, this form of cell death could serve as a potential therapeutic target.

Heliox has been used in respiratory medicine for decades [12,13]. It is produced by replacing nitrogen in the air (~78%) with helium, and supplementing with 21% oxygen. The density of heliox is one-third that of normal air density [14]. Furthermore, heliox preconditioning has been shown to have a neuroprotective effect by upregulating anti-oxidases and inhibiting necroptosis [15]. However, the specific processes underlying heliox's protection against IR damage as well as its potential link to ferroptosis are still not fully understood.

In the current study, an oxygen-glucose deprivation/reoxygenation (OGD/R) procedure was used to produce a cellular model of IR injury in the SH-SY5Y cell, a human neuroblastoma cell line. OGD/R-induced ferroptosis in these cells was then investigated using several techniques. Specifically, heliox produced a significant protective effect against OGD/R-induced ferroptosis in SH-SY5Y cells by activating the phosphatidylinositol 3-kinase/protein kinase B (PI3K/AKT) pathway.

2. Materials and Methods

2.1 Cell Culture

SH-SY5Y cells (IM-H227) which had been tested and validated for mycoplasma (See **Supplementary Material**) were purchased from Xiamen IMMOCELL Biotechnology Co., Ltd. (Xiamen, China) and cultured in 45% Dulbecco's modified eagle's medium (DMEM; 11965092, GIBCO, New York, NY, USA) and 45% Ham's F12 medium (11765054, GIBCO) with 10% fetal bovine serum (FBS; 10099141C, GIBCO) in an incubator at 37 °C and with 5% CO_2.

2.2 OGD/R and Heliox Treatment

When the SH-SY5Y cell density reached 70–80%, cells were washed three times using phosphate buffered solution (PBS) to completely remove the medium and then cultured in 50% glucose-free DMEM (11966025, GIBCO) and 50% Ham's F12 medium in an incubator at 37 °C for 4 h with 95% N_2 and 5% CO_2. The cells were then cultured in 45% DMEM containing glucose and 45% Ham's F12 medium with 10% FBS in an incubator containing 95% atmosphere and 5% CO_2 for 3, 6, 12, and 24 h, or in an incubator containing 80% helium and 20% oxygen for 12 and 24 h. Alternatively, cells were cultured for 24 h in 45% DMEM containing glucose and 45% Ham's F12 medium with 10% FBS and 5 µM MK-2206 2HCl (HY-10358, MedChemExpress, Monmouth Junction, NJ, USA) in an incubator containing 80% helium and 20% oxygen.

2.3 Cell Viability Assay

Medium (100 µL) containing 1×10^4 SH-SY5Y cells was cultured in a 96-well plate. After OGD/R and heliox treatment, 10 µL 5% methyl thiazolyl tetrazolium (MTT) was added to each well and the plate was incubated for 3 h at 37 °C. The medium was then carefully discarded and 100 µL dimethyl sulfoxide (DMSO, catalog number: 0219605580, MP Biomedicals, Santa Ana, CA, USA) was added to each well. The plate was incubated on a shaker at 70–80 rpm for 10 min. At 490 nm, an optical density (OD) measurement was made using a microplate reader (model: Varioskan LUX, Thermo Fisher Scientific, Waltham, MA, USA).

2.4 Determination of Malondialdehyde, Reduced Glutathione, Oxidized Glutathione Disulfide, and Fe^{2+} Levels

SH-SY5Y cells were lysed on ice in radioimmunoprecipitation assay (RIPA, catalog number: E-BC-R327, Elabscience, Wuhan, Hubei, China) buffer for 20 min. Centrifugation at 15,000 ×g for 10 min was then used to separate the supernatant. The malondialdehyde (MDA) assay kit (S0131S, Beyotime Biotechnology, Shanghai, China), reduced glutathione (GSH) and oxidized glutathione disulfide (GSSG) assay kit (S0053, Beyotime Biotechnology), and cell iron content assay kit (BC5315, Solarbio Life Sciences, Beijing, China) were used to quantify the concentrations of MDA, GSH, GSSG, and ferrous ion (Fe^{2+}), respectively, in the supernatant following the manufacturer's instructions. The relative levels of MDA, GSH, GSSG, and Fe^{2+} were calculated by comparing the OD value with the standard curve and normalizing according to the cell number.

2.5 Measurement of Reactive Oxygen Species

Following OGD/R or heliox treatment, reactive oxygen species (ROS) levels in SH-SY5Y cells were assessed using the 10 µM 2′,7′-Dichlorodihydrofluorescein diacetate (DCFH-DA, catalog number: 50101ES01, Yeason, Shanghai, China) fluorescence probe for 20 min at 37 °C in an incubator. The fluorescence signals from SH-SY5Y cells were measured at 560 nm using flow cytometry.

2.6 Mitochondrial Membrane Potential Measurement

After treatment under different conditions, the JC-1 probe (C2006, Beyotime Biotechnology) was used to determine mitochondrial membrane potential (MMP) in SH-SY5Y cells for 20 min at 37 °C in an incubator. PBS was used to wash the cells twice and flow cytometry was used to measure the fluorescence signals from SH-SY5Y cells.

2.7 Quantitative Polymerase Chain Reaction

The RNA, separated from SH-SY5Y cells using TRIzol reagent (Invitrogen, Waltham, MA, USA), was used for cDNA synthesis using a reverse transcription kit (R323-01, Vazyme, Nanjing, Jiangsu, China). The SYBR Master Mix (Q411-02, Vazyme) was used to carry out the quantitative polymerase chain reaction (qPCR). Each sample was analyzed in triplicate on an Applied Biosystems™ real-time fluorescent quantitative PCR system (model: 7500 Fast, Thermo Fisher Scientific). The following steps were used for the reaction: step I, 95 °C for 30 sec; step II, 40 cycles of 95 °C for 10 sec and 60 °C for 30 sec; and step III, 95 °C for 15 sec, 60 °C for 60 sec, and 95 °C for 15 sec. Data were analyzed using the $2^{-\Delta\Delta Ct}$ method. Primer sequences are shown in Table 1.

2.8 Immunoblotting

Following treatment under different conditions, SH-SY5Y cells were lysed by incubation on ice for 20 min in RIPA buffer containing phosphatase inhibitor. A bicinchoninic acid (BCA) kit (PA115-02; TIANGEN Biotechnology, Beijing, China) was used to extract proteins and measure their concentration. Equal protein amounts were loaded into the wells of a 10% sodium dodecyl sulfate-polyacrylamide (SDS-PAGE) gel. Electrophoresis was carried out at 80 V for 0.5 h and at 120 V for 1 h. At 350 mA for 3 h, the isolated proteins were deposited onto polyvinylidene fluoride membranes. Five percent non-fat milk was used to inhibit the membranes for 1 h. After being exposed to primary antibodies overnight at 4 °C, the mem-

Table 1. Primers for qPCR.

Gene	Forward primer (5′-3′)	Reverse primer (5′-3′)
ACSL4	GCTATCTCCTCAGACACACCGA	AGGTGCTCCAACTCTGCCAGTA
COX2	CGGTGAAACTCTGGCTAGACAG	GCAAACCGTAGATGCTCAGGGA
FTH1	TGAAGCTGCAGAACCAACGAGG	GCACACTCCATTGCATTCAGCC
GPX4	ACAAGAACGGCTGCGTGGTGAA	GCCACACACTTGTGGAGCTAGA
SLC7A11	TCCTGCTTTGGCTCCATGAACG	AGAGGAGTGTGCTTGCGGACAT
18S	CGACGACCCATTCGAACGTCT	CTCTCCGGAATCGAACCCTGA
PI3K	GAAGCACCTGAATAGGCAAGTCG	GAGCATCCATGAAATCTGGTCGC
AKT	TGGACTACCTGCACTCGGAGAA	GTGCCGCAAAAGGTCTTCATGG

qPCR, quantitative polymerase chain reaction; COX2, cyclooxygenase-2; FTH1, ferritin heavy chain 1; GPX4, glutathione peroxidase 4; PI3K, phosphatidylinositol 3-kinase; AKT, protein kinase B.

Table 2. Antibodies used for immunoblotting.

Classification	Antibodies	Manufacturer, city, state, country	Catalog number	Dilution
Primary antibody	SLC7A11	Proteintech, Wuhan, China	26864-1-AP	1:3000
	COX2	Proteintech, Wuhan, China	66351-1-Ig	1:3000
	ACSL4	Proteintech, Wuhan, China	22401-1-AP	1:3000
	FTH1	Abcam, Shanghai, China	ab183781	1:3000
	GPX4	Proteintech, Wuhan, China	67763-1-Ig	1:3000
	GAPDH	Proteintech, Wuhan, China	60004-1-Ig	1:5000
	P-PI3K	Cell Signaling technology, Boston, MA, USA	17366	1:3000
	PI3K	Proteintech, Wuhan, China	20584-1-AP	1:3000
	P-AKT	Proteintech, Wuhan, China	80455-1-RR	1:3000
	AKT	Proteintech, Wuhan, China	60203-2-Ig	1:3000
	P-p65	Abcam, Shanghai, China	ab76302	1:3000
	P65	Proteintech, Wuhan, China	80979-1-RR	1:3000
	P-p50	Abcam, Shanghai, China	Ab28849	1:3000
Secondary antibody	HRP-conjugated goat anti-rabbit IgG	Proteintech, Wuhan, China	SA00001-2	1:10,000
	HRP-conjugated goat anti-mouse IgG	Proteintech, Wuhan, China	SA00001-1	1:10,000

HRP, horse radish peroxidase; FTH, ferritin heavy chain.

branes were incubated with secondary antibody for 1 h at 25 °C. An enhanced chemiluminescence kit (WP20005, Thermo Fisher Scientific) was used to detect the protein bands, which were imaged using a Bio-Rad ChemiDoc MP imaging system (catalog number: 12003154, Bio-Rad, Hercules, CA, USA). All antibodies used are listed in Table 2.

2.9 Statistical Analysis

The creation of bar charts and statistical analysis were performed using GraphPad Prism (version 8.0, GraphPad Software, Inc., San Diego, CA, USA). Student's *t*-test (unpaired) and one-way analysis of variance (ANOVA) were used to compare parametric data between two groups and among multiple groups, respectively. Western blots were scanned and the signal intensity was quantified using ImageJ (version 2, National Institutes of Health, Bethesda, MD, USA). Statistical significance was determined at the following probability levels: $*p < 0.05$, $**p < 0.01$, $***p < 0.001$, and $****p < 0.0001$.

3. Results

3.1 OGD/R Inhibits the Survival of SH-SY5Y Cells

To examine the effect of heliox on IR injury, oxygen-glucose deprivation (OGD) was initially applied for 4 h to SH-SY5Y cells which were followed by incubation with oxygen and glucose for 0, 3, 6, 12, or 24 h. Using the MTT assay, a significant reduction in the SH-SY5Y cells' survival was observed following treatment with oxygen and glucose for 3, 6, 12, and 24 h (Fig. 1A). DCFH-DA staining and flow cytometry were performed to investigate ROS production after OGD/R treatment. The peak shifted to the right (Fig. 1B), indicating the mean fluorescence intensity (MFI) of DCFH-DA increased after reoxygenation for 3, 6, 12, and 24 h. As shown in Fig. 1C, ROS levels in SH-SY5Y cells treated with OGD/R also increased significantly. The JC-1 probe was used to investigate whether OGD/R treatment altered the MMP. As shown in Fig. 1D, OGD/R treatment of SH-SY5Y cells resulted in a noticeable increase in the proportion of cells displaying green fluorescence. The green/red ratio increased significantly with longer treatment

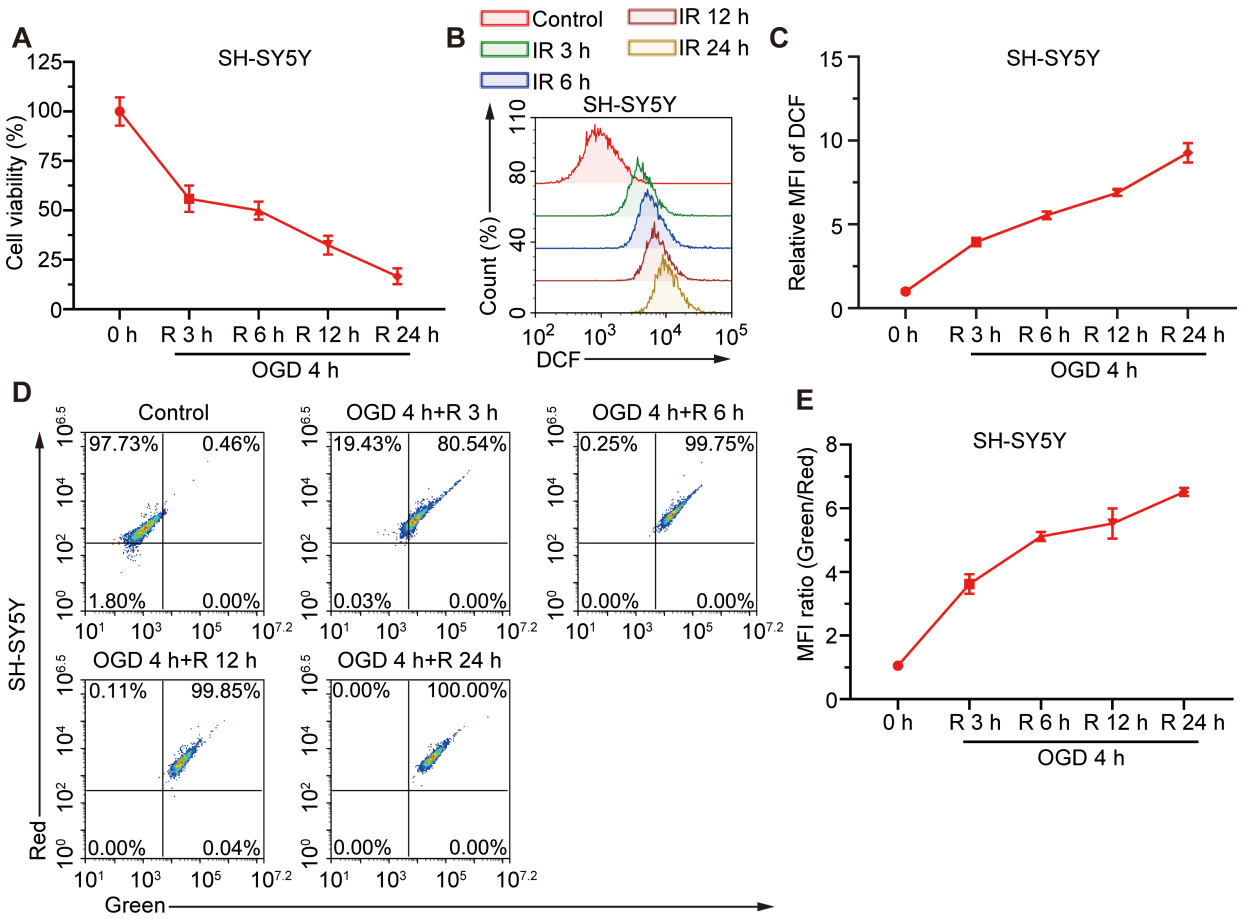

Fig. 1. OGD/R prevents SH-SY5Y cells from surviving. 4-h OGD exposure was applied to SH-SY5Y cells, which were followed by treatment with oxygen-glucose for 0, 3, 6, 12, or 24 h. Cell survival was then evaluated using the MTT assay (A); the DCFH-DA dye was used to gauge ROS generation (B); the relative mean fluorescence intensity (MFI) of the DCFH-DA probe was quantified (C); the MMP was determined using JC-1 dye and flow cytometry (D); and the MFI of JC-1 fluorescence was quantified (E). OGD denotes oxygen-glucose deprivation, and R represents reoxygenation. IR, ischemia/reperfusion; OGD, oxygen-glucose deprivation; OGD/R, oxygen-glucose deprivation/reoxygenation; MTT, methyl thiazolyl tetrazolium; DCFH-DA, 2′,7′-Dichlorodihydrofluorescein diacetate; ROS, reactive oxygen species; DCF, 2′,7′-Dichlorodihydrofluorescein diacetate.

times (Fig. 1E). OGD/R therefore decreased the survival and MMP of SH-SY5Y cells, and increased the production of ROS.

3.2 Heliox Protects OGD/R-Treated SH-SY5Y Cells from Ferroptosis

High ROS production occurs when cells undergo ferroptosis [16]. The above results indicate that OGD/R induces a large amount of ROS production in SH-SY5Y cells, suggesting that it may inhibit cell survival by inducing ferroptosis. In addition, heliox has been shown to protect the brain from acute focal IR injury [17]. To investigate the molecular mechanism by which heliox protects the brain, we therefore studied its role in ferroptosis. OGD/R-treated SH-SY5Y cells were cultured with helium and oxygen for 0, 12, or 24 h. Untreated cells acted as the controls. The ischemia reperfusion/helium-oxygen mixture (IR/HOM) 0 h group were cells that were cultured for 4 h under OGD and then for 6 h in 5% CO_2 and 95% air. The levels of ferroptosis markers [18], including *COX2*, *ACSL4, FTH1*, *SLC7A11*, *GPX4*, MDA, GSSG, and GSH, were all evaluated. OGD/R treatment of SH-SY5Y cells resulted in elevated levels of *COX2*, *ACSL4*, *FTH1*, MDA, GSSG, and Fe^{2+}; decreased levels of *SLC7A11*, *GPX4*, and GSH; and a lower GSH to GSSG (GSH/GSSG) ratio (Fig. 2A–H). Administration of heliox attenuated these OGD/R-induced effects. Moreover, the viability of OGD/R-treated cells increased significantly with heliox treatment (Fig. 2I). Furthermore, heliox treatment attenuated the increased generation of ROS observed in OGD/R-treated SH-SY5Y cells (Fig. 2J–K). JC-1 staining indicated that heliox treatment also significantly reversed the decrease in mitochondrial potential caused by OGD/R (Fig. 2L–M). In summary, heliox treatment reversed OGD/R-induced ferroptosis in SH-SY5Y cells.

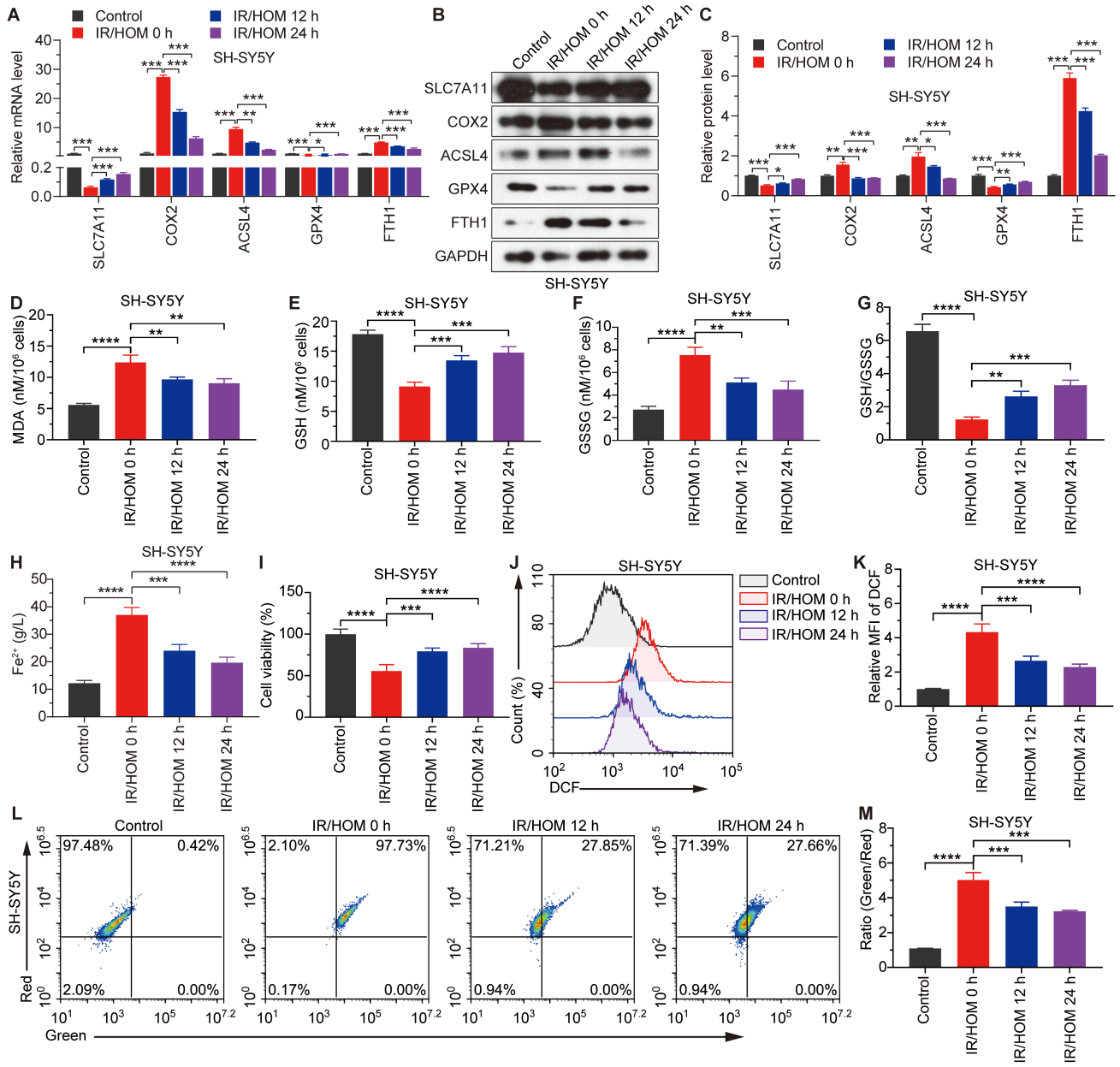

Fig. 2. Heliox protects OGD/R-treated SH-SY5Y cells from ferroptosis. OGD was applied to SH-SY5Y cells for 4 h, followed by heliox-glucose therapy for 0, 12, or 24 h. Assessments were then made of the mRNA (A) and protein levels (B,C) for COX2, ACSL4, FTH1, SLC7A11, and GPX4 using qPCR and immunoblotting, respectively. Commercial kits were used to measure MDA, GSH, GSSG, and Fe^{2+} levels, and the GSH to GSSG ratio (D–H). In order to gauge cell vitality, the MTT test was performed (I). DCFH-DA staining was used to detect ROS generation (J–K). MMP was assessed using the JC-1 probe and analyzed by flow cytometry (L–M). IR/HOM, ischemia reperfusion/helium-oxygen mixture; MDA, malondialdehyde; GSH, glutathione; GSSG, oxidized glutathione disulfide; Fe^{2+}, ferrous ion. *$p < 0.05$, **$p < 0.01$, ***$p < 0.001$, and ****$p < 0.0001$.

3.3 Heliox Activates the PI3K/AKT Pathway and Inhibits the NF-κB Pathway in OGD/R-Treated SH-SY5Y Cells

The PI3K/AKT pathway is known to play a crucial role in regulating cell proliferation [19]. Experiments were therefore conducted to evaluate the expression of proteins involved in the PI3K/AKT pathway following heliox treatment. Heliox treatment markedly upregulated the expression levels of phosphorylated PI3K and phosphorylated AKT in OGD/R-treated SH-SY5Y cells (Fig. 3A,B). Moreover, the mRNA levels of *PI3K* and *AKT* decreased after OGD/R exposure, but increased after heliox treatment (Fig. 3C). The levels of p50 and phosphorylated p65 were markedly increased in OGD/R-treated SH-SY5Y cells, but decreased significantly following heliox treatment (Fig. 3A,B). These findings suggest that heliox treatment effectively suppresses the nuclear factor-κB (NF-κB) path-

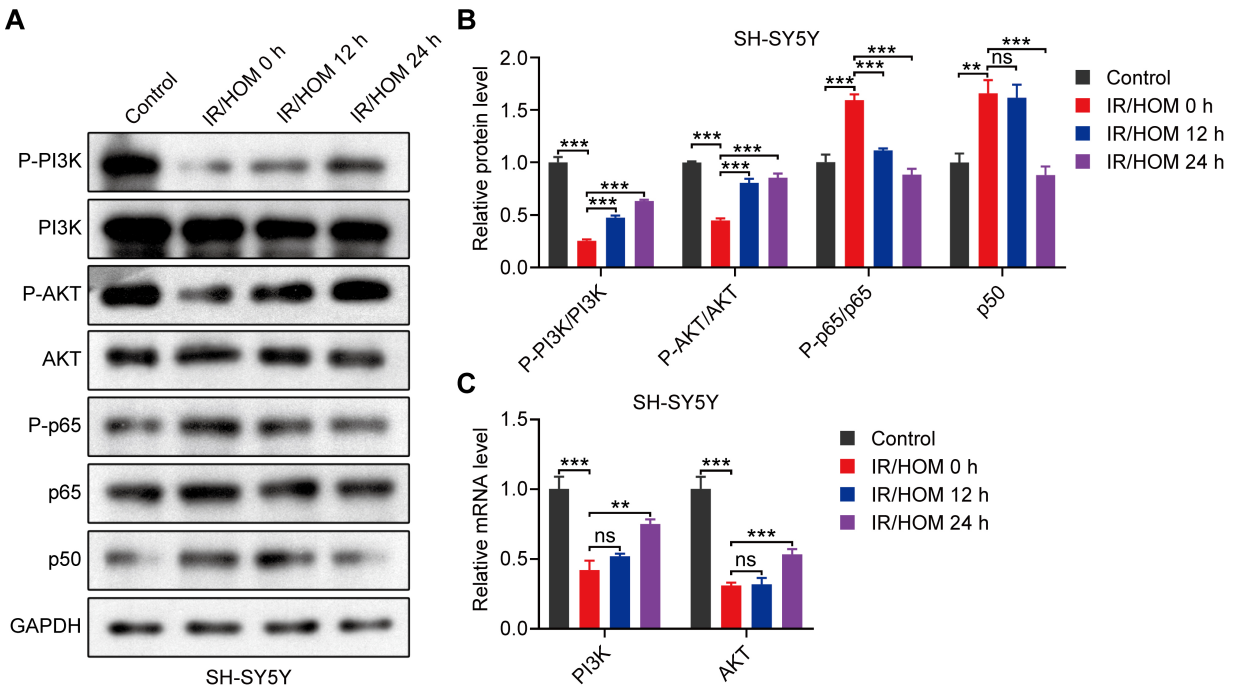

Fig. 3. Heliox therapy stimulates the PI3K/AKT pathway while impairing the NF-κB pathway in OGD-treated SH-SY5Y cells. OGD was applied to SH-SY5Y cells for 4 h, and then heliox-glucose was applied for 0, 12, or 24 h. The protein levels for P-PI3K, PI3K, P-AKT, AKT, P-p65, p65, p50, and GAPDH were then measured using immunoblotting (A,B), while the mRNA levels for *PI3K* and *AKT* were quantified using qPCR (C). ns, not significant. $^{**}p < 0.01$, $^{***}p < 0.001$.

way. Thus, heliox activates the PI3K/AKT pathway and inhibits the NF-κB pathway in OGD-treated SH-SY5Y cells.

3.4 Heliox Prevents Ferroptosis in SH-SY5Y Cells via Triggering the PI3K/AKT Pathway

After heliox administration for 24 h, we introduced the AKT inhibitor MK-2206 to OGD/R-treated SH-SY5Y cells to test if heliox exerts its protective effect via activation of the PI3K/AKT pathway. MK-2206 treatment significantly reduced the protein levels of phosphorylated AKT, SLC7A11, and GPX4 in heliox-treated SH-SY5Y cells (Fig. 4A,B). The decrease in MDA, GSSG, and Fe^{2+} levels in heliox-treated cells was reversed by MK-2206, while the increased GSH level and GSH to GSSG ratio was attenuated by MK-2206 (Fig. 4C–H). In heliox-treated SH-SY5Y cells, MK-2206 also decreased the viability and the MMP and increased ROS production (Fig. 4I–L). Heliox prevented ferroptosis in SH-SY5Y cells by stimulating the PI3K/AKT pathway.

4. Discussion

IR injury elicits a wide range of cellular and molecular responses within the brain, highlighting its significant pathological impact. To date, there are no effective therapies for the treatment of cerebral IR injury [20]. Experimental OGD/R treatment has been widely used to mimic IR injury [21]. The SH-SY5Y cell line is the most widely used model to investigate neuronal function [22–26]. By administering OGD/R to SH-SY5Y cells, we therefore created a cellular model of IR injury. In contrast to previous studies, the current investigation focused on the role of ferroptosis in OGD/R-treated SH-SY5Y cells.

OGD can cause SH-SY5Y cell death and increase intracellular ROS production [26]. In support of this, we also found that OGDs can induce ferroptosis and increase ROS production in SH-SY5Y cells. Other studies have shown that OGD leads to lower cellular expression of ferritin heavy chain (FTH) [27,28]. However, we found that FTH expression increased in OGD-treated SH-SY5Y cells. Increased FTH was also reported in hippocampal neurons treated with 0.5 µM erastin [29]. Ferritin plays an antioxidant role in cells by isolating redox-active iron [30]. During ferroptosis, nuclear receptor coactivator 4-mediated ferritin autophagy produces a large amount of ferrous ion and consumes large amounts of ferritin [31]. The resulting cellular imbalance may activate protective mechanisms to replenish ferritin; we therefore speculate that the up-regulation of FTH may be a compensatory mechanism for iron homeostasis. However, it might also instigate a chain reaction that results in cell death. These conjectures need further investigation.

There is increasing evidence that ferroptosis is halted when the PI3K-AKT pathway is activated. In SH-SY5Y cells, OGD reduced activity in the PI3K-AKT pathway, while heliox reversed this inhibition, thus reducing cell damage caused by OGD. Moreover, the NF-κB and PI3K-

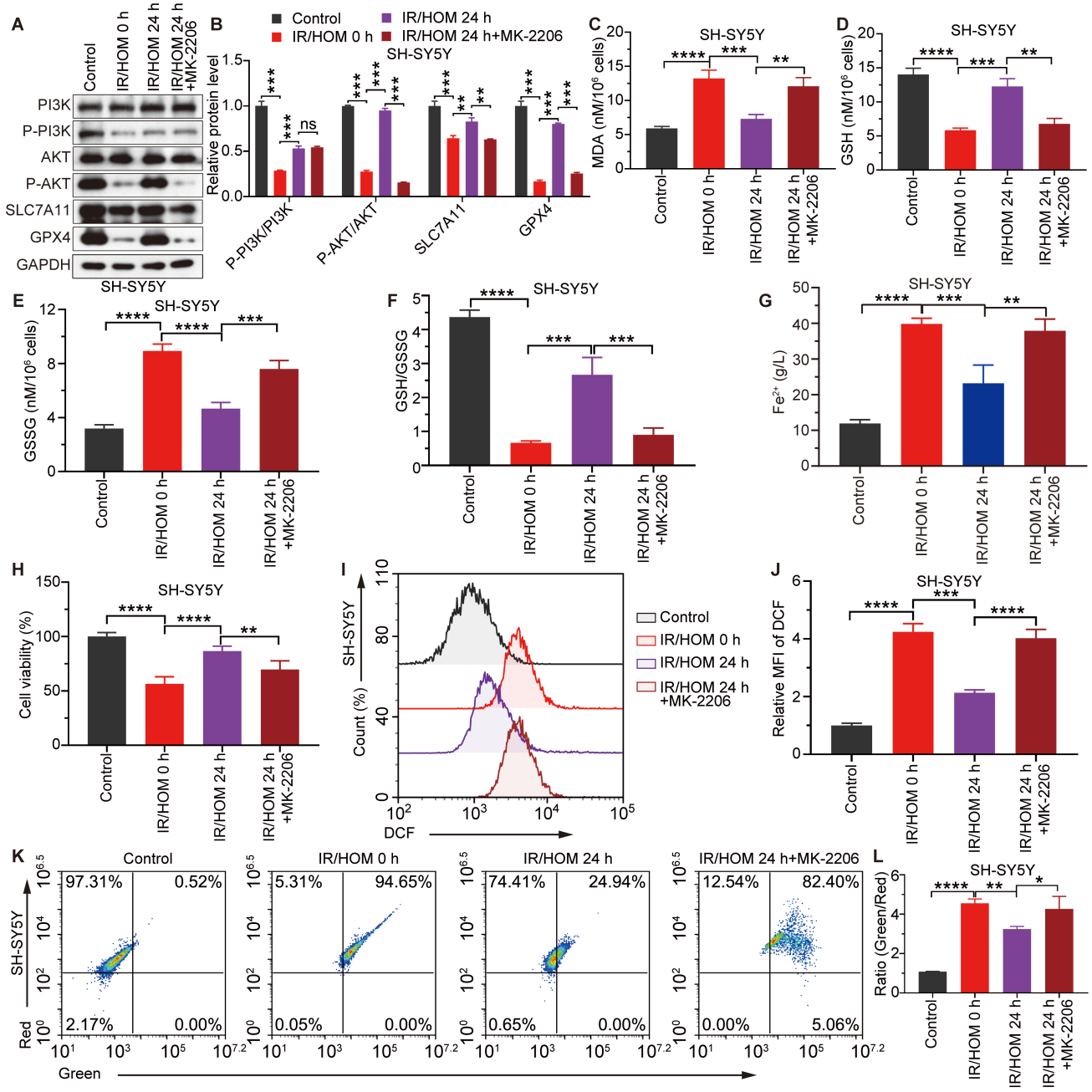

Fig. 4. Heliox protects SH-SY5Y cells from ferroptosis via triggering the PI3K/AKT pathway. After oxygen-glucose deprivation for 4 h, SH-SY5Y cells were treated with heliox-glucose and MK-2206 for 0 or 24 h. The following assessments were then made: protein levels for P-PI3K, PI3K, P-AKT, AKT, SLC7A11, and GPX4 using immunoblotting (A,B); levels of MDA, GSH, GSSG, and Fe^{2+}, and the GSH to GSSG (GSH/GSSG) ratio using commercial kits (C–G); cell viability using the MTT assay (H); ROS levels using the DCFH-DA probe (I,J); and MMP using the JC-1 probe and flow cytometry (K–L). ns, not significant. *$p < 0.05$, **$p < 0.01$, ***$p < 0.001$, and ****$p < 0.0001$.

AKT pathways are interconnected and play crucial roles in cellular signaling. The PI3K-AKT pathway can exert inhibitory effects on NF-κB activity, while NF-κB can in turn influence the PI3K-AKT pathway [32]. Furthermore, heliox inhibited the NF-κB pathway in OGD-treated SH-SY5Y cells. Heliox-mediated inactivation of the NF-κB signaling pathway in SH-SY5Y cells therefore further enhanced its protective effects against IR injury. A similar mechanism has been reported for melatonin treatment [33].

The current study had some limitations. Although we confirmed that blocking of the NF-κB pathway by heliox and OGD/R treatment was followed by inflammation, the inflammatory response requires further study, including investigating whether heliox can reduce the expression of pro-

inflammatory factors. Second, only one cell model of IR injury was employed to assess the protective impact of heliox *in vitro*. An animal model of IR injury is required to validate the *in vivo* therapeutic value of heliox and its mechanism of action [34].

5. Conclusions

In summary, the current findings demonstrate that OGD/R in SH-SY5Y cells induces ferroptosis, enhances ROS levels, promotes lipid peroxidation, and diminishes antioxidant capacity. Heliox treatment can, however, effectively reverse these effects by activating the PI3K/AKT pathway. These findings suggest that heliox could be a promising innovative therapeutic approach for the treatment of IR injury.

Availability of Data and Materials

The data that support the findings of this study are available within the article.

Author Contributions

SY and WX designed the research study. SY, WX, WJX, and YFC performed the experiments. SY, WX and WJX analyzed the data. SY and WJX drafted the manuscript. All authors contributed to editorial changes in the manuscript. All authors read and approved the final manuscript. All authors have participated sufficiently in the work and agreed to be accountable for all aspects of the work.

Ethics Approval and Consent to Participate

Not applicable.

Acknowledgment

Not applicable.

Funding

Xiamen medical and health guiding project [3502Z20224ZD1056] provided financial support for this study.

Conflict of Interest

The authors declare no conflict of interest.

Supplementary Material

Supplementary material associated with this article can be found, in the online version, at https://doi.org/10.31083/j.jin2301014.

References

[1] Yellon DM, Hausenloy DJ. Myocardial reperfusion injury. New England Journal of Medicine. 2007; 357: 1121–1135.

[2] Eltzschig HK, Eckle T. Ischemia and reperfusion–from mechanism to translation. Nature Medicine. 2011; 17: 1391–1401.

[3] Sun Z, Zhao T, Lv S, Gao Y, Masters J, Weng H. Dexmedetomidine attenuates spinal cord ischemia-reperfusion injury through both anti-inflammation and anti-apoptosis mechanisms in rabbits. Journal of Translational Medicine. 2018; 16: 209.

[4] Pefanis A, Ierino FL, Murphy JM, Cowan PJ. Regulated necrosis in kidney ischemia-reperfusion injury. Kidney International. 2019; 96: 291–301.

[5] Shi B, Ma M, Zheng Y, Pan Y, Lin X. mTOR and Beclin1: Two key autophagy-related molecules and their roles in myocardial ischemia/reperfusion injury. Journal of Cellular Physiology. 2019; 234: 12562–12568.

[6] Qu Y, Liu Y, Zhang H. ALDH2 activation attenuates oxygen-glucose deprivation/reoxygenation-induced cell apoptosis, pyroptosis, ferroptosis and autophagy. Clinical and Translational Oncology. 2023. (online ahead of print)

[7] Yang Y, Klionsky DJ. Autophagy and disease: unanswered questions. Cell Death and Differentiation. 2020; 27: 858–871.

[8] Dixon SJ, Lemberg KM, Lamprecht MR, Skouta R, Zaitsev EM, Gleason CE, *et al*. Ferroptosis: an iron-dependent form of non-apoptotic cell death. Cell. 2012; 149: 1060–1072.

[9] Farmer EE, Mueller MJ. ROS-mediated lipid peroxidation and RES-activated signaling. Annual Review of Plant Biology. 2013; 64: 429–450.

[10] Scindia PhD Y, Leeds Md J, Swaminathan Md S. Iron Homeostasis in Healthy Kidney and its Role in Acute Kidney Injury. Seminars in Nephrology. 2019; 39: 76–84.

[11] Zhao Y, Xin Z, Li N, Chang S, Chen Y, Geng L, *et al*. Nanoliposomes of lycopene reduces ischemic brain damage in rodents by regulating iron metabolism. Free Radical Biology and Medicine. 2018; 124: 1–11.

[12] Rodrigo G, Pollack C, Rodrigo C, Rowe BH. Heliox for nonintubated acute asthma patients. Cochrane Database of Systematic Reviews. 2006: CD002884.

[13] Chen X, Li J, Kang R, Klionsky DJ, Tang D. Ferroptosis: machinery and regulation. Autophagy. 2021; 17: 2054–2081.

[14] Martinón-Torres F. Noninvasive ventilation with helium-oxygen in children. Journal of Critical Care. 2012; 27: 220.e1–e9.

[15] Li Y, Liu K, Kang ZM, Sun XJ, Liu WW, Mao YF. Helium preconditioning protects against neonatal hypoxia-ischemia via nitric oxide mediated up-regulation of antioxidases in a rat model. Behavioural Brain Research. 2016; 300: 31–37.

[16] Dixon SJ, Stockwell BR. The role of iron and reactive oxygen species in cell death. Nature Chemical Biology. 2014; 10: 9–17.

[17] Pan Y, Zhang H, Acharya AB, Cruz-Flores S, Panneton WM. The effect of heliox treatment in a rat model of focal transient cerebral ischemia. Neuroscience Letters. 2011; 497: 144–147.

[18] Stockwell BR, Jiang X, Gu W. Emerging Mechanisms and Disease Relevance of Ferroptosis. Trends in Cell Biology. 2020; 30: 478–490.

[19] Chen JT, Schmidt L, Schürger C, Hankir MK, Krug SM, Rittner HL. Netrin-1 as a Multitarget Barrier Stabilizer in the Peripheral Nerve after Injury. International Journal of Molecular Sciences. 2021; 22: 10090.

[20] Krishnamurthi RV, Feigin VL, Forouzanfar MH, Mensah GA, Connor M, Bennett DA, *et al*. Global and regional burden of first-ever ischaemic and haemorrhagic stroke during 1990-2010: findings from the Global Burden of Disease Study 2010. The Lancet Global Health. 2013; 1: e259–e281.

[21] Zhang ZG, Zhang QZ, Cheng YN, Ji SL, Du GH. Antagonistic effects of ultra-low-molecular-weight heparin against cerebral ischemia/reperfusion injury in rats. Pharmacological Reports. 2007; 56: 350–355.

[22] Sallmon H, Hoene V, Weber SC, Dame C. Differentiation of human SH-SY5Y neuroblastoma cells by all-trans retinoic acid activates the interleukin-18 system. Journal of Interferon and Cytokine Research. 2010; 30: 55–58.

[23] Marko DM, Foran G, Vlavcheski F, Baron DC, Hayward GC, Baranowski BJ, *et al*. Interleukin-6 Treatment Results in GLUT4 Translocation and AMPK Phosphorylation in Neuronal SH-SY5Y Cells. Cells. 2020; 9: 1114.

[24] Chandan G, Ganguly U, Pal S, Singh S, Saini RV, Chakrabarti SS, *et al*. GLUT inhibitor WZB117 induces cytotoxicity with increased production of amyloid-beta peptide in SH-SY5Y cells preventable by beta-hydroxybutyrate: implications in Alzheimer's disease. Pharmacological Reports. 2023; 75: 482–489.

[25] Russo VC, Kobayashi K, Najdovska S, Baker NL, Werther GA. Neuronal protection from glucose deprivation via modulation of glucose transport and inhibition of apoptosis: a role for the insulin-like growth factor system. Brain Research. 2004; 1009: 40–53.

[26] Wang HF, Wang ZQ, Ding Y, Piao MH, Feng CS, Chi GF, *et al*. Endoplasmic reticulum stress regulates oxygen-glucose deprivation-induced parthanatos in human SH-SY5Y cells via improvement of intracellular ROS. CNS Neuroscience and Therapeutics. 2018; 24: 29–38.

[27] Zhang F, Li Z, Gao P, Zou J, Cui Y, Qian Y, *et al*. HJ11 decoction restrains development of myocardial ischemia-reperfusion injury in rats by suppressing ACSL4-mediated ferroptosis. Frontiers in Pharmacology. 2022; 13: 1024292.

[28] Liu H, Zhao Z, Yan M, Zhang Q, Jiang T, Xue J. Calycosin decreases cerebral ischemia/reperfusion injury by suppressing ACSL4-dependent ferroptosis. Archives of Biochemistry and Biophysics. 2023; 734: 109488.

[29] Hanke N, Rami A. Inhibition of autophagy rescues HT22 hippocampal neurons from erastin-induced ferroptosis. Neural Regeneration Research. 2023; 18: 1548–1552.

[30] Fang Y, Chen X, Tan Q, Zhou H, Xu J, Gu Q. Inhibiting Ferroptosis through Disrupting the NCOA4-FTH1 Interaction: A New Mechanism of Action. ACS Central Science. 2021; 7: 980–989.

[31] Santana-Codina N, Gikandi A, Mancias JD. The Role of NCOA4-Mediated Ferritinophagy in Ferroptosis. Advances in Experimental Medicine and Biology. 2021; 1301: 41–57.

[32] Oeckinghaus A, Ghosh S. The NF-kappaB family of transcription factors and its regulation. Cold Spring Harbor perspectives in biology. 2009; 1: a000034.

[33] Zhi SM, Fang GX, Xie XM, Liu LH, Yan J, Liu DB, *et al*. Melatonin reduces OGD/R-induced neuron injury by regulating redox/inflammation/apoptosis signaling. European Review for Medical and Pharmacological Sciences. 2020; 24 :1524–1536.

[34] Taheri F, Sattari E, Hormozi M, Ahmadvand H, Bigdeli MR, Kordestani-Moghadam P, *et al*. Dose-Dependent Effects of Astaxanthin on Ischemia/Reperfusion Induced Brain Injury in MCAO Model Rat. Neurochemical Research. 2022; 47: 1736–1750.